Quantum transport through a Z-shaped silicene nanoribbon*

A Ahmadi Fouladi†

Department of Physics, Sari Branch, Islamic Azad University, Sari, Iran

(Received 18 November 2016; revised manuscript received 16 January 2017; published online 20 February 2017)

In this work, the electronic transport properties of Z-shaped silicene nanoribbon (ZsSiNR) structure are investigated. The calculations are based on the tight-binding model and Green's function method in Landauer–Büttiker formalism, in which the electronic density of states (DOS), transmission probability, and current–voltage characteristics of the system are calculated, numerically. It is shown that the geometry of the ZsSiNR structure can play an important role to control the electron transport through the system. It is observed that the intensity of electron localization at the edges of the ZsSiNR decreases with the increase of the spin-orbit interaction (SOI) strength. Also, the semiconductor to metallic transition occurs by increasing the SOI strength. The present theoretical results may be useful to design silicene-based devices in nanoelectronics.

Keywords: Z-shaped silicene nanoribbon, electronic transport, Green's function method, spin–orbit interaction

PACS: 73.23.–b, 73.63.–b **DOI:** 10.1088/1674-1056/26/4/047304

1. Introduction

Silicene, a monolayer honeycomb lattice of silicon atoms, has been recently synthesized[1–4] and has attracted intensive interest because of its unique physical properties. Also, the compatibility of silicene with the existing silicon-based semiconductor technology has stimulated researchers to investigate its electronic properties. Very recently, Tao *et al.* fabricated a silicene-based field effect transistor at room temperature.[5] Silicene has a slightly buckled structure and relatively large spin–orbit interaction (SOI).[6] Due to this buckled structure, the band-gap of silicene can be modulated by an external perpendicular electric field.[7] Silicene nanoribbons (SiNRs) can be good candidates for possible electronic and spintronic devices because they have a tunable band gap depending on the size and geometry. Using first principles calculations, Ding and Ni[8] have shown that the armchair silicene nanoribbons (ASiNRs), similar to the graphene nanoribbons (GNRs) can be metals or semiconductors depending on width $n_{\rm w}$. The ASiNRs are metallic for $n_{\rm w} = 3m+2$ (where m is a positive integer), otherwise the ASiNRs are semiconductors. Also, they have found that the antiferromagnetic semiconductor is the ground state for zigzag SiNR (ZSiNR) and it becomes half-metal under transverse electric field. Since the experimental realization of patterned GNRs,[9] GNR nano-junctions of various shapes such as Z-shaped,[10] L-shaped,[11] T-shaped,[12] S and U-shaped[13] junctions based on the zigzag and armchair GNRs with interesting physical properties have been proposed, and their electronic transport properties have been studied.[10–18] Inspired by these GNR-based junctions, various shapes of SiNRs with unique physical properties can be proposed. Recently, the electron transport properties of SiNRs have been investigated.[19–23]

In this paper, we numerically investigate the electronic transport properties of the Z-shaped SiNR (ZsSiNR) structure composed of a middle junction connected to two semi-infinite armchair SiNR leads in the coherent regime. The model of such a structure is shown schematically in Fig. 1. Here, we put emphasis on the geometry of the ZsSiNR structure and spin–orbit interaction (SOI), and obtain the density of states (DOS), transmission probability, and current–voltage characteristics, using the Green's function method in the framework of a tight-binding model in Landauer–Büttiker formalism. The results show that the electron transport properties of the system strongly depend on geometry of ZsSiNR and SOI strength.

The rest of this paper is organized as follows: in Section 2, we give a model and the description of the method. In Section 3, the numerical results and discussion are presented, followed by a conclusion in Section 4.

2. Methodology

Let us consider a ZsSiNR system consists of a middle junction connected to two left and right armchair SiNR leads, as shown in Fig. 1. Relying on Landauer–Büttiker formula based on the non-equilibrium Green's function method, we evaluate the current as a function of the applied bias voltage[24]

$$I(V) = \frac{2e}{h}\int_{-\infty}^{+\infty} T(E)\left[f_{\rm L} - f_{\rm R}\right]{\rm d}E, \tag{1}$$

where $f_{\rm L(R)} = f(E-\mu_{\rm L(R)})$ is the Fermi distribution function of the left (right) lead with chemical potential $\mu_{\rm L(R)} = E_{\rm F} \pm (eV/2)$ and Fermi energy $E_{\rm F}$. The transmission probability $T(E)$ as a function of the injecting electron energy E,

*Project supported by the Sari Branch, Islamic Azad University, Iran (Grant No. 1-24850.

†Corresponding author. E-mail: a.ahmadifouladi@iausari.ac.ir

© 2017 Chinese Physical Society and IOP Publishing Ltd

can be expressed in terms of the Green's function of the middle junction and the coupling of the middle junction with two left and right leads by the expression:

$$T(E) = \mathrm{Tr}\,[\Gamma_{\mathrm{L}}(E)\,G(E)\,\Gamma_{\mathrm{R}}(E)\,G^{\dagger}(E)], \tag{2}$$

where G is the Green's function of the middle junction which can be written as

$$G(E) = \left[(E+\mathrm{i}\eta)I - H_{\mathrm{m}} - \Sigma_{\mathrm{L}}(E) - \Sigma_{\mathrm{R}}(E)\right]^{-1}, \tag{3}$$

where $\eta \to 0^{+}$ is an infinitesimal value, I is the identity matrix and $\Sigma_{\mathrm{L(R)}}$ is the self-energy of the left (right) SiNR lead due to the coupling of the middle junction with left and right leads that can be calculated by the recursive method described by Sancho and co-workers.[25] Using the tight-binding approximation, the Hamiltonian of the middle junction can be written as follows:[26]

$$H_{\mathrm{m}} = -t_0 \sum_{\langle ij\rangle\alpha} c^{\dagger}_{i\alpha} c_{j\alpha} + \mathrm{i}\frac{\lambda_{\mathrm{SO}}}{3\sqrt{3}} \sum_{\langle\langle ij\rangle\rangle\alpha\beta} \eta_{ij}\, c^{\dagger}_{i\alpha}\, \varsigma^{z}_{\alpha\beta}\, c_{j\beta} - \mathrm{i}\frac{2}{3}\lambda_{\mathrm{R}} \sum_{\langle\langle ij\rangle\rangle\alpha\beta} \xi_{ij}\, c^{\dagger}_{i\alpha}\, (\boldsymbol{\sigma}\times \boldsymbol{d}^{0}_{ij})^{z}_{\alpha\beta}\, c_{j\beta}, \tag{4}$$

where $c^{\dagger}_{i\alpha}$ ($c_{j\beta}$) creates (annihilates) an electron with spin polarization α (β) at site i (j) in SiNR lattice. $\langle ij\rangle$ and $\langle\langle ij\rangle\rangle$ stand for the nearest-neighbor and next nearest-neighbor pairs in the SiNR lattice, respectively. The first term of the above equation shows the usual nearest-neighbor hopping integral with a transfer energy $t_0 = 1.6$ eV.[26] In the second and the third terms, the effective intrinsic spin–orbit interaction (SOI) parameter and the intrinsic Rashba SOI parameter are $\lambda_{\mathrm{SO}} = 3.9$ meV and $\lambda_{\mathrm{R}} = 0.7$ meV, respectively.[26] $\boldsymbol{\sigma} = (\sigma_x, \sigma_y, \sigma_x)$ is the Pauli matrix with $\eta_{ij} = -1$ ($\eta_{ij} = +1$) if the next-nearest neighbor hopping is clockwise (anticlockwise) with respect to the positive z axis, and $\xi_{ij} = +1$ ($\xi_{ij} = -1$) for A (B) site. $\boldsymbol{d}^{0}_{ij} = \boldsymbol{d}_{ij}/|\boldsymbol{d}_{ij}|$ is the unit vector parallel to the vector $\boldsymbol{d}_{ij}$ connecting the two sites i and j in the same sublattice. In the absence of SOI terms, the Hamiltonian H_{m} is similar to the case of GNR. In Eq. (2), $\Gamma_{\mathrm{L(R)}} = \mathrm{i}(\Sigma_{\mathrm{L(R)}} - \Sigma^{\dagger}_{\mathrm{L(R)}})$ is the coupling function due to the coupling of the middle junction with the left (right) lead. Finally, the average density of state (ADOS) and the local density of state (LDOS) can be calculated by the following equations[24]

$$\mathrm{ADOS}(E) = -(1/N\pi)\,\mathrm{Tr}\,[\mathrm{Im}(G(E))], \tag{5}$$

$$\mathrm{LDOS}(E) = -(1/\pi)\,\mathrm{Im}(G(E)). \tag{6}$$

where N is the number of silicon atoms in the middle junction.

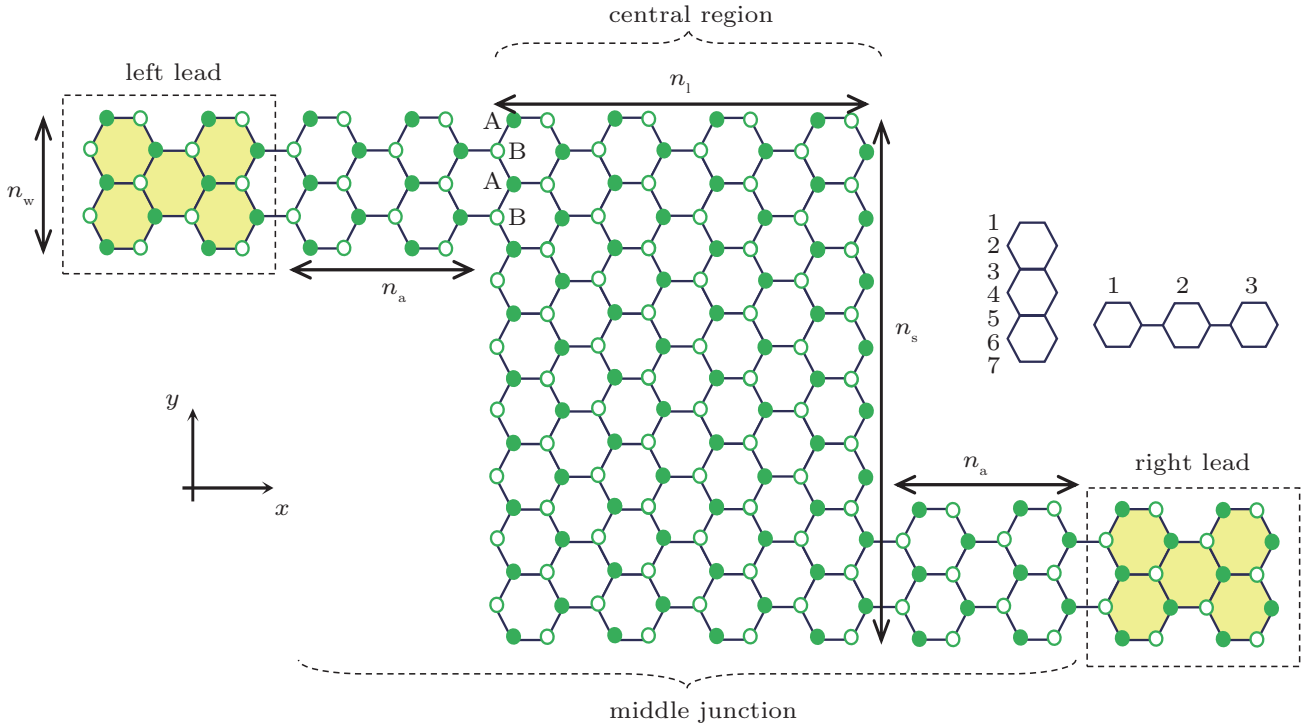


Fig. 1. (color online) Schematic representation of a ZsSiNR structure composed of a middle junction attached to two semi-infinite armchair SiNR leads. The silicon atoms belong to the two distinct sublattices, A and B. Here, $n_{\mathrm{w}} = 5$, $n_{\mathrm{a}} = 2$, $n_{\mathrm{s}} = 17$, and $n_{\mathrm{l}} = 4$.

3. Results and discussion

In this section, we describe numerical results obtained from the above theoretical prescription given in Section 2 to investigate the electron transport properties of the ZsSiNR system. We set $E_{\mathrm{F}} = 0$, $T = 11$ K. Throughout the analysis we use $\lambda_{\mathrm{SO}} = 3.9$ meV, except for Fig. 4 where λ_{SO} is varying. First, the dependence of transport properties of the ZsSiNR structure on the central region width (n_{s}) with $n_{\mathrm{w}} = 5$, $n_{\mathrm{a}} = 2$, $n_{\mathrm{l}} = 4$, is shown in Figs. 2(a)–2(c). In Figs. 2(a) and 2(b), we have shown

the transmission probability and the ADOS of the ZsSiNR system as a function of the incident electron energy for different n_s, respectively.

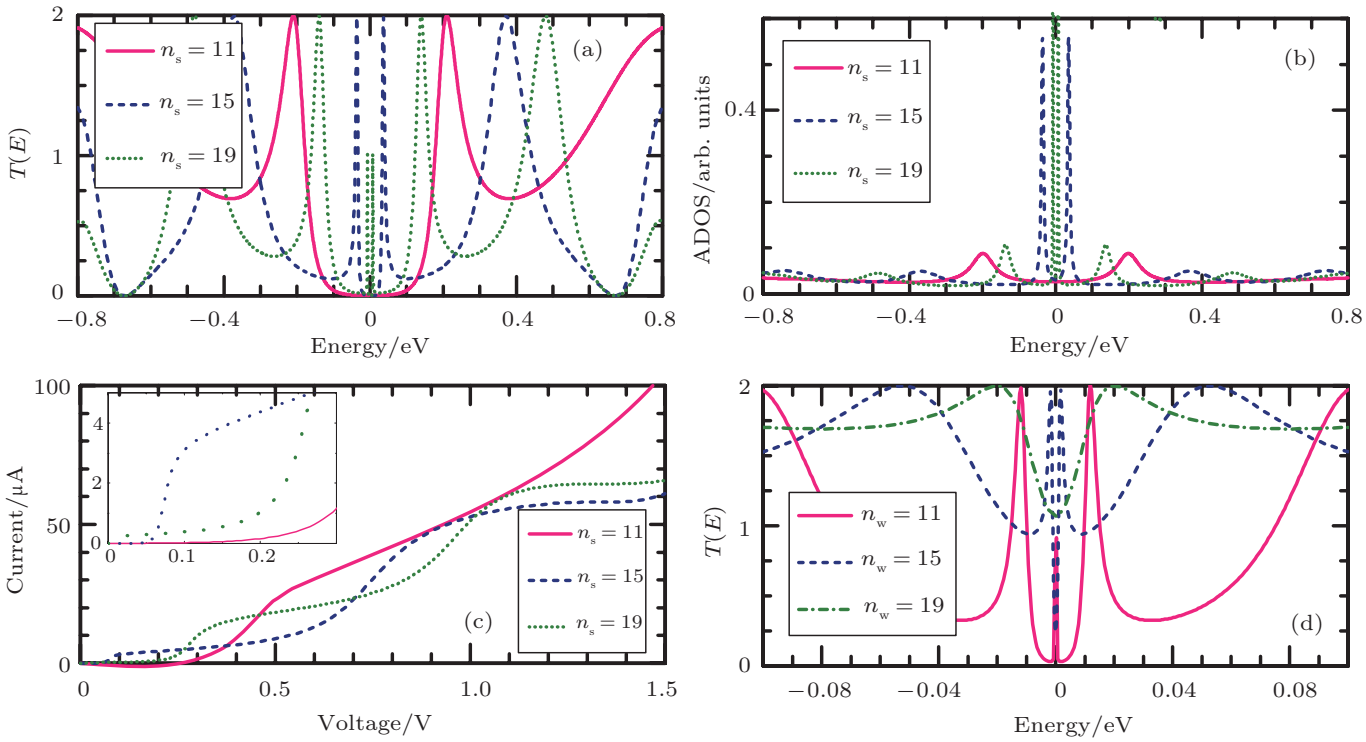


Fig. 2. (color online) (a) The transmission probability and (b) the ADOS of the ZsSiNR system as a function of the incident electron energy with $n_w = 5$, $n_a = 2$, $n_l = 4$ for different central region widths n_s: $n_s = 11$ (solid curve), $n_s = 15$ (short dashed curve), $n_s = 19$ (short dotted curve). (c) Current–voltage (I–V) characteristic of the ZsSiNR system for different n_s. (d) The transmission probability as a function of the incident electron energy with $n_s = 31$, $n_a = 2$, $n_l = 5$ for different widths of the SiNR electrodes n_w.

From Fig. 2(a), we can see that the resonant peaks are symmetrically located at the two sides of the Dirac point ($E = 0$) in the transmission probability spectrum. These resonant peaks are narrowed as they approach the Dirac point. For $n_s = 11$ there is a transmission gap and the system shows the semiconducting behavior. With the increase of the n_s, the transmission gap decreases and the system tends toward the metallic behavior. This semiconducting to metallic transition is more apparent for the larger λ_{SO}. The peaks of ADOS represent the location where the incident energy is resonant with respect to the ZsSiNR states (see Fig. 2(b)). It is noticeable that by increasing the n_s, the height of ADOS peaks near the Dirac point increases, while the transmission peaks are suppressed, which demonstrates that the resonant peaks are induced by the quasi-bound states confined in the ZsSiNR structure. Besides, for all values of the n_s, the ADOS at the Dirac point have nonzero value, while the transmission probability is almost zero. It shows that the energy eigenstate at the Dirac point is localized. Also, there are several zero transmission dips for ZsSiNR structure, which are related to the anti-resonances caused by the destructive interference between propagating states along the ribbon and the bound states localized in the ZsSiNR system. We calculated the current–voltage (I–V) characteristic of the ZsSiNR structure with different central region widths and the results are plotted in Fig. 2(c). It is clearly observed that a threshold voltage is needed to generate current through the system for all different central region widths, which shows that, at low bias voltages the system is in an off-state. With increasing n_s, the value of the threshold voltage decreases (see inset of Fig. 2(c)). This behavior is due to a decrease in the transmission gap with the increase of the n_s. With the increase in bias voltage, the electrochemical potentials in the left and right electrodes cross one of the energy levels of the ZsSiNR structure, and consequently a current channel is opened up and a jump in the I–V curve is seen. The current exhibits a step-like behavior due to the existence of the resonant peaks in the bias window. The sharpness and the height of these current steps depend on the width and the height of the transmission peaks. The currents have smooth steps due to the broadening of the quantized states. As we increase n_s, the height of the first current step decreases and also, the number of current steps increases due to the fact that more resonance peaks appear in the transmission spectrum.

In Fig. 2(d) the effect of the SiNR electrodes width (n_w) on the transmission function of the system with $n_a = 2$, $n_l = 5$, $n_s = 31$, is investigated. As can be seen, the transmission gap completely disappears with the increase of n_w. In fact the number of channels for the electron transport processes increases by increasing of n_w, hence the average transmission

probability increases.

The effect of the central region length, n_l, on the transport properties of the ZsSiNR structure, with $n_w = 5$, $n_a = 2$, and $n_s = 13$, is investigated and the results are plotted in Fig. 3. From Fig. 3(a), it is seen that the transmission peaks and dips are narrowed and move toward the Dirac point, as we increase n_l. For the case of $n_l = 3$, the transmission probability at the Dirac point has nonzero value and accordingly, the system represents the metallic behavior. With the increase of the n_l, the transmission probability tends to zero at the Dirac point, and the metal to semiconductor transition occurs. The increase of the height of the ADOS peaks with the increase of the n_l is shown in Fig. 3(b). The ADOS values at the Dirac point are nonzero (similar to Fig. 2(b)), while the transmission probability tends to zero as we increase the n_l. It shows that the localization of the energy eigenstate at the Dirac point increases with the enhancement of the n_l. Also, the ADOS value at the Dirac point decreases as we increase n_l. The I–V curves of the ZsSiNR structure in terms of the n_l are shown in Fig. 3(c). For the case of $n_l = 3$, there is no threshold voltage which shows that, the system is in an on-state (see inset of Fig. 3(c)). With the increase of the n_l, a threshold voltage appears and therefore, the system is turned off at low bias voltages.

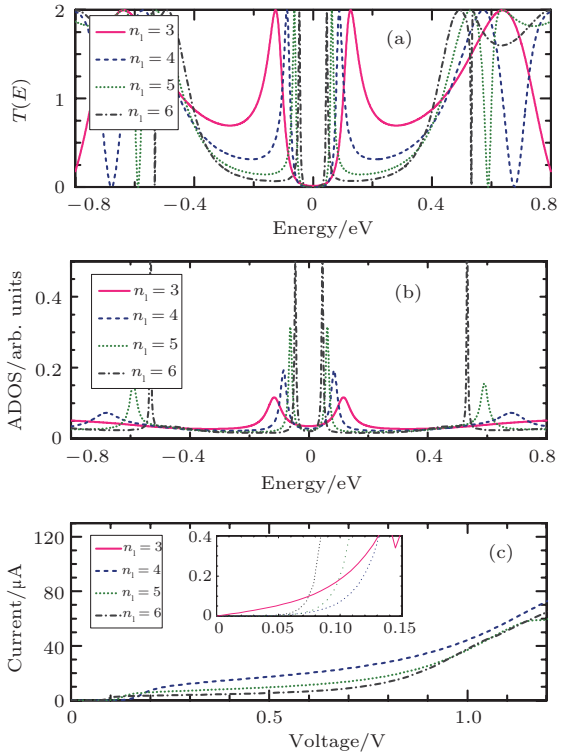


Fig. 3. (color online) (a) The transmission probability and (b) the ADOS of the ZsSiNR system as a function of the incident electron energy with $n_w = 5$, $n_a = 2$, $n_s = 13$ for different central region lengths n_l: $n_l = 3$ (solid curve), $n_l = 4$ (short dashed curve), $n_l = 5$ (short dotted curve), $n_s = 6$ (short dashed–dotted curve). (c) The I–V curve of the ZsSiNR system for different n_s.

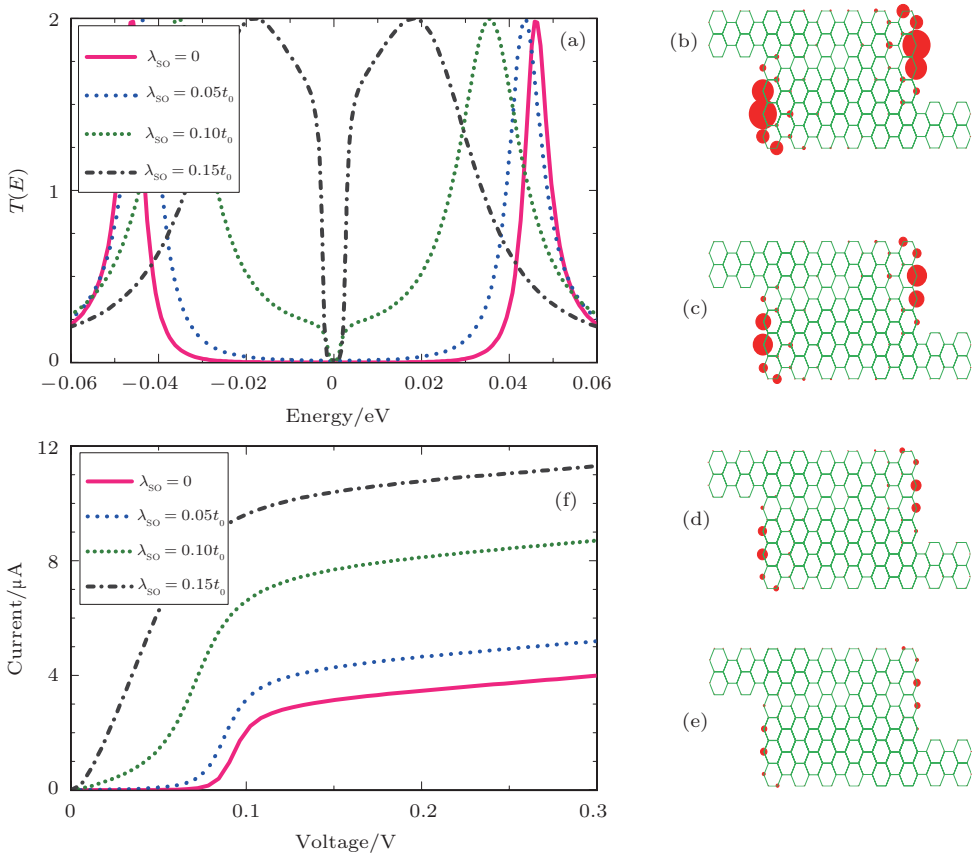


Fig. 4. (color online) (a) The transmission probability and of the ZsSiNR system as a function of the incident electron energy with $n_w = 5$, $n_a = 2$, $n_s = 13$, $n_l = 6$ for different values of the λ_{SO}: $\lambda_{SO} = 0$ (solid curve), $\lambda_{SO} = 0.05t_0$ (short dashed curve), $\lambda_{SO} = 0.1t_0$ (short dotted curve), $\lambda_{SO} = 0.15t_0$ (short dashed–dotted curve). The spatial-resolved LDOS of ZsSiNR junction at the transmission peaks with (b) $\lambda_{SO} = 0$, $E = 46$ meV; (c) $\lambda_{SO} = 0.05t_0$, $E = 43$ meV; (d) $\lambda_{SO} = 0.1t_0$, $E = 35$ meV, and (e) $\lambda_{SO} = 0.15t_0$, $E = 18$ meV. (f) The I–V curve of the ZsSiNR system for different values of λ_{SO}.

In Fig. 4, we demonstrate the dependence of the transport properties of the ZsSiNR structure on the effective SOI parameter, λ_{SO}, with $n_w = 5$, $n_a = 2$, $n_s = 13$, and $n_l = 6$. The results show that the transmission gap decreases when λ_{SO} is increased from 0 to $0.15t_0$ (see Fig. 4(a)), and the semiconductor to metal transition occurs. This transition depends on the geometry of the system. The dependence of the band gap of the SiNR on the width and λ_{SO} has been investigated in Ref. [27]. When λ_{SO} increases, the transmission peaks are broadened and move toward the Dirac point. To gain better insight into the effect of λ_{SO} on the electron transport properties of ZsSiNR structure, the spatial-resolved LDOS corresponding to the resonant peaks with the energies $E = 46$,meV, 43 meV, 35 meV, and 18 meV are plotted in Figs. 4(b)–4(e), respectively. As can be seen from Fig. 4(b), for $\lambda_{SO} = 0$, the electrons in the ZsSiNR structure are strongly localized at the isolated sites on the edges, which is similar to the results from the Z-shaped GNR,[10] and accordingly, the transmission peak is sharp. As we increase the λ_{SO}, the intensity of electron localization at the edges decreases, and hence, the broadening of the transmission peaks increases. The I–V curves of the ZsSiNR junction for different values of the λ_{SO} are presented in Fig. 4(f). It is observed that, by increasing the λ_{SO}, in addition to the increasing of the current's height due to the broadening and enhancement of transmission peaks, the threshold voltage decreases, leading to off-state to on-state transition. Consequently, our model predicts SOI-controlled switching between on and off-states.

It is noteworthy that the ZsSiNR junction composed of the zigzag SiNR components reveals the metallic nature for different values of SOI strength, length and width of the system. Therefore, the ZsSiNR junction composed of the armchair SiNR components is more desirable to fabricate switching devices.

4. Conclusion

Using the non-equilibrium Green's function method and within the framework of the tight-binding Hamiltonian model in Landauer–Büttiker formalism, we have investigated the electron transport properties of ZsSiNR system formed by a middle junction sandwiched between two semi-infinite armchair SiNR leads. We have shown that the electron transport properties of the system are very sensitive to the geometric structure and SOI strength. With the increase of the central region and SiNR electrodes widths, the transmission gap decreases and the system tends toward the metallic behavior, and consequently, the value of the threshold voltage decreases. By increasing the central region length, the transmission probability at the Dirac point tends to zero, and the metal to semiconductor transition occurs, and accordingly, a threshold voltage appears in I–V curve. Also, the results show that the transmission gap decreases with the increase of the SOI strength and therefore, the threshold voltage decreases, leading to off-state to on-state transition. The results might have significant applications in controlling the electron transport in silicene-based nanoelectronic devices.

References

[1] Vogt P, De Padova P, Quaresima C, Avila J, Frantzeskakis E, Asensio M C, Resta A, Ealet B and Le Lay G 2012 *Phys. Rev. Lett.* **15** 155501
[2] Aufray B, Kara A, Vizzini S, Oughaddou H, Léandri C, Ealet B and Le Lay G 2010 *Appl. Phys. Lett.* **96** 183102
[3] Lalmi B, Oughaddou H, Enriquez H, Kara A, Vizzini S, Ealet B and Aufray B 2010 *Appl. Phys. Lett.* **97** 223109
[4] Lin C L, Arafune R, Kawahara K, Tsukahara N, Minamitani E, Kim Y, Takagi N and Kawai M 2012 *Appl. Phys. Express* **5** 045802
[5] Tao L, Cinquanta E, Chiappe D, Grazianetti C, Fanciulli M, Dubey M, Molle A and Akinwande D 2015 *Nat. Nano* **10** 227
[6] Liu C C, Feng W and Yao Y 2011 *Phys. Rev. Lett.* **107** 076802
[7] Ezawa M 2012 *New J. Phys.* **14** 033003
[8] Ding Y and Ni J 2009 *Appl. Phys. Lett.* **95** 083115
[9] Han M Y, Ozyilmaz B, Zhang Y and Kim P 2007 *Phys. Rev. Lett.* **98** 206805
[10] Chen Y P, Xie Y E and Zhong J 2008 *Phys. Lett. A* **372** 5928
[11] Chen Y P, Xie Y E and Yan X H 2008 *J. Appl. Phys.* **103** 063711
[12] Chen Y P, Xie Y E, Sun L Z and Zhong J 2008 *Appl. Phys. Lett.* **93** 092104
[13] Zhang Z Z, Wu Z H, Chang K and Peeters F M 2009 *Nanotechnology* **20** 415203
[14] Li H, Liu N, Zheng Y, Wang F and Hao H 2010 *Physica B: Conden. Matter* **405** 3316
[15] Xu J G, Wang L and Weng M Q 2013 *J. Appl. Phys.* **114** 153701
[16] Tong H and Wu M W 2012 *Phys. Rev. B* **85(20)** 205433
[17] Ahmadi Fouladi A and Ketabi S 2015 *Physica E: Low-dimensional Systems and Nanostructures* **74** 475
[18] Ahmadi Fouladi A 2016 *Superlattices and Microstructures* **95** 108-114
[19] Zhou B, Zhou B, Zeng Y, Zhou G and Duan M 2016 *Phys. Lett. A* **380** 1469
[20] Zhou B, Zhou B, Zeng Y, Zhou G and Duan M 2016 *Phys. Lett. A* **380** 282
[21] Wang X S, Shen M, An X T and Liu J J 2016 *Phys. Lett. A* **380** 1663
[22] Trivedi S, Srivastava A and Kurchania R 2014 *J. Comput. Theor. Nanosci.* **11** 789
[23] Shakouri Kh, Simchi H, Esmaeilzadeh M, Mazidabadi H, and Peeters F M 2015 *Phys. Rev. B* **92** 035413
[24] Datta S 1995 *Electronic Transport in Mesoscopic Systems* (Cambridge: Cambridge University Press)
[25] Sancho M P L, Sancho J M L, Sancho J M L and Rubio J 1985 *J. Phys. F: Met. Phys.* **15** 851
[26] Liu C C, Jiang H and Yao Y 2011 *Phys. Rev. B* **84** 195430
[27] Ezawa M and Nagaosa N 2013 *Phys. Rev. B* **88** 121401